Atom-optical gratings induced by multiphoton excitation of electronic Rydberg wave packets

G. Alber and W. T. Strunz

Fakultät für Physik, Albert-Ludwigs-Universität, D-79104 Freiburg im Breisgau, Germany
(Received 31 March 1994)

The formation of atom-optical gratings induced by multiphoton excitation of Rydberg states is discussed for fast atoms. With the help of semiclassical path-integral methods the correlation between the dynamics of a laser-excited Rydberg electron and the momentum transferred to the atomic center of mass in a spatially modulated laser field is exhibited quantitatively. These types of laser excitation processes might offer new perspectives for the realization of atomic multiple beam splitters and for atom-lithographic applications.

Atom optics is rapidly emerging as a new field in atomic and optical physics. Taking advantage of the wave aspects of the atomic center-of-mass motion, a major effort in this field of research is directed towards the development of analogues of optical instruments in which the role of photons is played by atoms. For the realization of basic atom-optical elements, such as atomic beam splitters or lenses, an understanding of the deflection of atoms by laser beams is of central importance [1–9]. Due to the large mass difference between an atomic nucleus and its electrons, momentum can be transferred from a laser field to the atomic center of mass essentially only by excitation of the internal electronic degrees of freedom [10]. The resulting strong correlation between the internal dynamics of an atom and its center-of-mass motion offers new perspectives both for the development of atom-optical instruments and the investigation of the dynamics of electrons in atoms.

An interesting example in this respect is the excitation of Rydberg states during the flight of an atom through a standing-wave laser field. In the case of a one-photon excitation process it has been shown recently that atomic beam deflection can be described theoretically in a convenient way with the help of semiclassical path representations [11]. Thereby the probability amplitude $a_g(x)$, for example, of finding an atom after the interaction with the laser field at position x in the initially prepared energetically low-lying bound state $|g\rangle$ is represented as a sum of elementary contributions associated with classical Coulomb paths of an excited Rydberg electron moving in the Coulomb field of the positively charged core. Depending on whether these elementary probability amplitudes overlap in time or not, either the *wave* or the *particle* aspects of the electronic dynamics prevail. A dominance of the wave aspects corresponds to the well-known two-level limit where only two bound atomic states are coupled almost resonantly by the laser field. The particle aspects manifest themselves if a large number of Rydberg states are excited coherently by laser-induced power broadening [12] and a radially localized electronic Rydberg wave packet is prepared. Thus a simple correspondence can be established between certain phase and amplitude modulations of state-selective atomic probability amplitudes produced by standing-wave laser fields, such as $a_g(x)$, and the corresponding electronic dynamics in the field of the positively charged ionic core. These spatial modulations manifest themselves in the diffraction of atoms by laser light in a way

that is similar to that in which the phase and amplitude gratings of optics manifest themselves in the diffraction of electromagnetic fields.

In this Rapid Communication it is shown that laser-induced excitation of Rydberg states via an intermediate, resonant bound state offers the possibility of generating a special class of phase and amplitude modulations of state-selective probability amplitudes. These modulations cannot be produced by one-photon excitation processes. They are caused by the simultaneous presence of particle *and* wave aspects of the dynamics of a laser-excited Rydberg electron. With their help, atomic multiple beam splitters might be realized which lead to large momentum transfers. Atomic beam splitters, which lead to similarly large momentum transfers but are based on a physically different mechanism, namely the so called "magneto-optical" effect, have been discussed recently by Adams *et al.* [4].

In order to analyze the basic physical aspects let us consider an idealized (effectively two-dimensional) atomic beam deflection setup, as shown schematically in Fig. 1(a). A monochromatic beam of atoms (total mass M, center-of-mass momentum $\vec{P}_{in}$), which are prepared in an energetically low-lying bound state $|g\rangle$, crosses a standing-wave laser field of the form $\vec{E}(x,t) = \Theta(y)\Theta(L-y)\vec{\mathscr{E}}(x)\exp(-i\omega t)$ +c.c. at right angles. [$\Theta(y)$ denotes the Heaviside function.] In the following discussion we concentrate on the important special case $\vec{\mathscr{E}}(x) = \vec{\mathscr{E}}_0\sin(kx)$. However, it should be men-
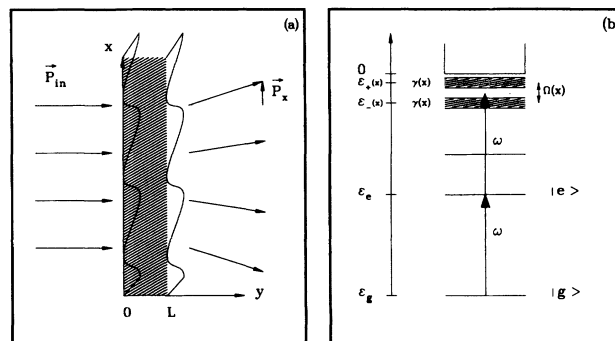

FIG. 1. Schematic representation of (a) the atomic beam diffraction setup and (b) the laser-induced excitation process considered. The squiggly lines indicate the standing-wave laser field.

<u>50</u>   R3577

tioned that our main results, i.e., Eqs. (1) and (5), are also valid for more general spatial dependences of the laser field. During the flight through the laser field each atom is excited to Rydberg states close to the photoionization threshold by two-photon excitation via an intermediate resonant bound state $|e\rangle$ [Fig. 1(b)]. Typically, thereby, the initially prepared state $|g\rangle$ is depleted. It is assumed in the following that the laser intensity is so small that ionization from the Rydberg states to continuum states well above threshold is negligible. To a good degree of approximation this is valid for moderate laser intensities I, which are much smaller than the atomic unit, i.e., $I \ll I_0 = 1.41 \times 10^{17}$ W cm^{-2} [12]. Furthermore, it is assumed that the atoms are so fast that their kinetic energy is much larger than the interaction energy with the laser field and that during the flight through the interaction region their motion along the standing wave is negligible, i.e., $kL(P_x/P_{\text{in}}) \ll 2\pi$ (Raman-Nath approximation). Therefore, approximately, the center of mass of an atom evolves freely on a straight-line trajectory, with $\tau = L/v_{\text{in}}$ denoting the time of flight through the laser field [10]. As for fast atoms, this time of flight can always be chosen much smaller than the radiative lifetime of the excited bound state $|e\rangle$. Effects of spontaneous emission of photons are neglected in the following. In this case the x dependence of the laser field leads to a characteristic x dependence of atomic probability amplitudes. Thus, for the excitation process shown in Fig. 1(b), the semiclassical path representation of the state-selective probability amplitude that a fast atom will enter and leave the laser field at position x in state $|g\rangle$ or $|e\rangle$ is given by [13]

$$a_j(x,\tau) = \frac{i}{2\pi} \int_{-\infty+i0}^{\infty+i0} d\epsilon \, e^{-i(\epsilon-\varphi_j)\tau} \langle j|(\epsilon-\mathcal{H})^{-1}|g\rangle$$

$$+ \sum_{N=1}^{\infty} \frac{\gamma}{2\pi} \int_{-\infty+i0}^{0} d\epsilon \, e^{-i(\epsilon-\varphi_j)\tau} \langle j|(\epsilon-\mathcal{H})^{-1}|e\rangle$$

$$\times (e^{2i\pi\nu}\chi)(\bar{\chi}\chi e^{2i\pi\nu})^{N-1} \langle e|(\epsilon-\mathcal{H})^{-1}|g\rangle, \quad (1)$$

with $\epsilon = -1/(2\nu^2)$, $j = g, e$, and $\varphi_g = 2\omega$, $\varphi_e = \omega$. (Hartree atomic units are used.)

The first term of Eq. (1), which is determined completely by the effective two-level Hamiltonian

$$\mathcal{H} = [\epsilon_g + 2\omega + \vec{P}_{\text{in}}^2/(2M)]|g\rangle\langle g|$$

$$+ [\epsilon_e + \omega + \vec{P}_{\text{in}}^2/(2M) + \delta\omega(x) - i\gamma(x)/2]|e\rangle\langle e|$$

$$+ \Omega(x)/2|e\rangle\langle g| + \Omega(x)^*/2|g\rangle\langle e|, \quad (2)$$

describes laser-induced depletion of the initial state $|g\rangle$ by one-photon resonant two-photon ionization via the intermediate resonant state $|e\rangle$. The Rabi frequency is given by $\Omega(x) = 2\langle e|\vec{\mu} \cdot \vec{\mathcal{E}}(x)|g\rangle$ with the atomic dipole operator $\vec{\mu}$. The quadratic Stark shift $\delta\omega(x)$ and the excitation rate $\gamma(x) = 2\pi|\langle \epsilon=0|\vec{\mu} \cdot \vec{\mathcal{E}}(x)|e\rangle|^2$ characterize the laser-induced coupling between the excited state $|e\rangle$ and the final Rydberg states close to threshold. Numerically, $\gamma(x)$ equals the ionization rate from state $|e\rangle$ to continuum states close to threshold according to the "golden rule." These quantities describe the laser-induced electronic excitation process which takes place in a reaction zone extending only a few

Bohr radii around the atomic nucleus. Compared with the large size of highly excited Rydberg states this reaction zone is well localized around the atomic nucleus.

The Nth term in Eq. (1) may be interpreted as the contribution of the Nth return of a laser-excited Rydberg electron to the reaction zone. The quantity $2\pi\nu$ is the classical action of a Rydberg electron of energy $\epsilon < 0$ which moves along a classical bound Coulomb orbit with near-zero angular momentum. With each return to the reaction zone a stimulated transition to one of the bound states $|g\rangle$ or $|e\rangle$ may take place, thus causing an increase of the probability amplitudes $a_g(x,\tau)$ and $a_e(x,\tau)$. Alternatively, with each return to the reaction zone, a Rydberg electron may be scattered resonantly by the laser field or by the ionic core. These scattering processes are described by the scattering matrix elements [13]

$$\bar{\chi} = 1 - i\gamma\langle e|(\epsilon - \mathcal{H})^{-1}|e\rangle \quad (3)$$

and $\chi = e^{2i\pi\alpha}$ [14] with the quantum defect α.

As apparent from Eq. (1) the periodic x dependence of the laser field leads to a corresponding spatial variation of the parameters $\Omega(x)$, $\delta\omega(x)$, and $\gamma(x)$ which characterize the atom-laser interaction. Therefore, during the flight of an atom through the laser field, the contribution of each return of a laser-excited Rydberg electron to the reaction zone centered around the atomic nucleus produces a characteristic phase and amplitude modulation in state-selective probability amplitudes. The corresponding probability amplitudes of the momentum distribution, which describes atomic diffraction, are obtained from such a phase and amplitude modulation by Fourier transform, [10] i.e.,

$$a_j(P_x, \tau) = \frac{k}{2\pi} \int_0^{2\pi/k} dx \, e^{-ixP_x} a_j(x,\tau), \quad (4)$$

with $P_x = \pm 2lk$ (l integer) for $j = g$ and $P_x = k \pm 2lk$ for $j = e$. Thus, the internal dynamics of an excited Rydberg electron which moves in the Coulomb field of the positively charged ionic core may be used in a controlled way to produce suitable phase and amplitude modulations. Alternatively these modulations of state-selective probability amplitudes or the corresponding momentum distribution of the scattered atoms may be used to investigate the dynamics of Rydberg electrons in atoms.

As a practical example let us consider a case in which Rydberg states are excited resonantly via the intermediate bound state $|e\rangle$. Furthermore, let us assume that the Rabi frequency of the bound-bound transition $|g\rangle \rightarrow |e\rangle$ is much larger than the field-induced ionization rate, i.e., $\gamma(x) \ll |\Omega(x)|$ [Fig. 1(b)]. Under these conditions Rydberg states in energy intervals of width $\gamma(x)$ around the mean energies $\epsilon_{\pm}(x) = \bar{\epsilon} \pm |\Omega(x)|/2 < 0$ with $\bar{\epsilon} = \epsilon_g + 2\omega$ are excited significantly. These mean excited energies correspond to one-photon transitions from the dressed atom-field states $|\pm\rangle$ of the resonantly coupled bound states $|g\rangle$ and $|e\rangle$. Assuming linear dependences of the effective quantum number ν on energy within each of these energy intervals of width $\gamma(x)$, Eq. (1) simplifies to

$$a_g(x,\tau) = e^{-i\phi} \frac{1}{2} \sum_{\pm} e^{\pm i|\Omega(x)|\tau/2} \left\{ e^{-i[\delta\omega(x)-i\gamma(x)/2]\tau/2} \right.$$

$$+ \sum_{N=1}^{\infty} \sum_{r=0}^{N-1} \binom{N-1}{r} \Theta(\tau - NT_{\pm}(x))$$

$$\times (\chi e^{2i\pi\bar{\nu}(x)_{\pm}})^N \frac{[-\gamma(x)(\tau - NT_{\pm}(x))/2]^{r+1}}{(r+1)!}$$

$$\left. \times e^{-i[\delta\omega(x)-i\gamma(x)/2](\tau - NT_{\pm}(x))/2} \right\} \qquad (5)$$

with $\phi = [\epsilon_g + \vec{P}_{in}^2/(2M)]\tau$. The effective quantum numbers of the mean excited Rydberg states are denoted $\bar{\nu}(x)_{\pm} = [-2\epsilon_{\pm}(x)]^{-1/2}$. An analogous expression can be derived for $a_e(x,\tau)$. Thereby $T_{\pm}(x)$ are the classical orbit times of Coulomb orbits of near-zero angular momentum and energies $\epsilon_{\pm}(x)$. Due to the spatial variation of the laser field, all these quantities depend on the position x at which an atom crosses the laser field. Equation (5) exhibits clearly the phase and amplitude modulations of the state-selective transition amplitude $a_g(x,\tau)$ which are produced by repeated returns of an excited Rydberg valence electron to the reaction zone centered around the atomic nucleus. Equation (5) together with its more general form given in Eq. (1) are the main results of this Rapid Communication.

The physical interpretation of the terms appearing in Eq. (5) is straightforward: Due to ac-Stark splitting between the resonantly coupled states $|g\rangle$ and $|e\rangle$ during the flight of an atom through the laser field, a Rydberg electron is excited either with mean energy $\epsilon_+(x)$ or $\epsilon_-(x)$. The probability amplitudes of these two pathways of excitation are denoted by the signs "$\pm$." The first term in curly brackets on the right hand side of Eq. (5) describes depletion of the initially prepared state $|g\rangle$ via these two pathways. The Nth term of the sum describes the contribution from the Nth return of an excited Rydberg electron to the reaction zone. With each return to this reaction zone a stimulated transition to the strongly coupled bound states $|e\rangle$ and $|g\rangle$ may take place. This leads to an increase of the state-selective probability amplitudes $a_g(x,\tau)$ and $a_e(x,\tau)$ at multiples of the mean classical orbit times $T_{\pm}(x)$ of the excited Rydberg states. As apparent from the Heaviside functions in Eq. (5) a contribution from the Nth return of an excited Rydberg electron with mean energy $\epsilon_{\pm}(x)$ can occur only if the time of flight of the atom through the laser field exceeds the N-fold of the corresponding mean classical orbit time, i.e., $\tau > NT_{\pm}(x)$. Furthermore, with each return to the reaction zone a Rydberg electron may be scattered by the core in the presence of the laser field. The integer r enumerates these possible scattering events, which may take place in the time interval $\tau = L/v_{in}$ between the initial excitation and final stimulated transition to one of the bound states $|e\rangle$ or $|g\rangle$. The binomial coefficient in Eq. (5) equals the number of r-fold laser-assisted scattering events that are possible during N returns of the excited Rydberg electron to the reaction zone.

In Fig. 2(a) the time evolution of the probability of observing an atom after its flight through the laser field either in state $|g\rangle$ or $|e\rangle$ is shown (full curve). The laser field is as-
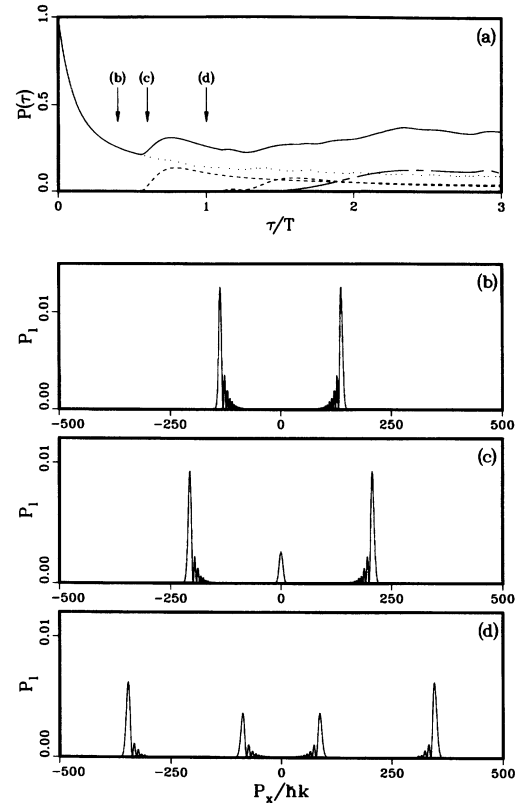

FIG. 2. Time evolution of total probability $P(\tau)$ (a) and momentum distributions $P_l(\tau)$ at times $\tau = 0.4T$ (b), $\tau = 0.6T$ (c), and $\tau = T$ (d), with $P(\tau) = \Sigma_l P_l(\tau)$ and $P_l(\tau) = |a_g(P_x,\tau)|^2 + |a_e(P_x,\tau)|^2$ ($P_x = lk$). The classical orbit time corresponding to the mean excited energy $\bar{\epsilon} = \epsilon_g + 2\omega = -10^{-5}$ a.u. is $T = 0.7 \times 10^8$ a.u. = 1.7 ns. The other parameters are: $\Omega_0 = 10^{-5}$ a.u., $\gamma_0 = 4 \times 10^{-7}$ a.u., and $\delta\omega(x) = 0$, $\alpha = 0$.

sumed to be of the form $\vec{\mathcal{E}}(x) = \vec{\mathcal{E}}_0 \sin kx$, with Ω_0 and γ_0 indicating the maximum values of Rabi frequency and ionization rate. In this example the energies of the excited Rydberg states are located sufficiently well below the ionization threshold so that effects of dispersion of the generated Rydberg wave packets can be neglected for the interaction times shown. If an atom crosses the standing-wave laser field at a position x at which the initial state $|g\rangle$ is depleted on a time scale small in comparison with the mean classical orbit times of the excited Rydberg states, i.e., $1/\gamma(x) \ll T_{\pm}(x)$, two radially localized electronic Rydberg wave packets with mean energies $\epsilon_{\pm}(x)$ are generated. The maxima appearing after the initial depletion of the bound states $|g\rangle$ and $|e\rangle$ in Fig. 2(a) are due to stimulated transitions of these electronic Rydberg wave packets to one of these bound states. These transitions take place during one of the subsequent returns of these wave packets to the reaction zone centered around the atomic nucleus. In the remaining curves inserted in Fig. 2(a) the separate contributions of the initial depletion of states $|g\rangle$ and $|e\rangle$ (dotted curve), the first and second returns of the faster electronic Rydberg wave packet (dashed curves), and the first return of the slower electronic Rydberg wave packet (chain dashed curve) are shown.

In Figs. 2(b–d) momentum distributions of atoms diffracted by the standing-wave laser field are shown for the

three interaction times that are indicated by arrows in Fig. 2(a). In Fig. 2(b) the interaction time τ between an atom and the laser field is so small that the electronic Rydberg wave packets have not yet returned to the atomic nucleus. Thus the momentum distribution shows characteristic features of one-photon resonant two-photon ionization in a standing-wave laser field. According to Eq. (5) the maxima of the momentum distribution appear approximately at the classical values $P_x = \pm (\hbar k)(\Omega_0 \tau/2)$. It is the Rabi oscillations between the bound states $|g\rangle$ and $|e\rangle$ which lead to the large momentum transfer in this case. The suppression of the oscillatory dependence on the transferred momentum, which is characteristic for two resonantly coupled states [10], originates from the depletion of the bound states $|g\rangle$ and $|e\rangle$. In Fig. 2(c) the time of flight τ is sufficiently large so that the faster Rydberg wave packet with mean energy $\epsilon_-(x)$ and mean orbit time $T_-(x)$ has just returned to the atomic nucleus. Thus the time $(\tau - T_-)$ available for stimulated transitions of this wave packet to one of the bound states $|g\rangle$ or $|e\rangle$ is not yet long enough to lead to a significant momentum transfer from the laser field to the atomic center of mass. Thereby, the quantity T_- is the smallest mean return time of all atoms that cross the laser field, i.e., $T_- = \min_x\{T_-(x)\}$. This implies that in the momentum distribution, in addition to the maxima originating from the initial depletion process, a maximum centered around $P_x \approx 0$ also appears. A further increase of the time of flight leads to a splitting of this central maximum as shown in Fig. 2(d). Now four well-pronounced maxima appear in the momentum distribution of the diffracted atoms. The two outermost peaks are due to depletion of the bound states. The central maxima now originate from the first return of the faster wave packet to the atomic nucleus. According to Eq. (5) these maxima appear approximately at the classical values $P_x = \pm (\hbar k)[\Omega_0 (\tau - T_-)/2]$.

The main features exhibited by these momentum distributions suggest the use of resonant multiphoton excitation of Rydberg states as a means for realizing atomic multiple beam splitters that split an atomic beam coherently into two or more parts and, in addition, lead to large momentum transfers. As far as the practical feasibility of such a beam splitter is concerned, let us consider the parameters used in Fig. 2 in more detail. The momentum splittings shown in Figs. 2(b–d) are achieved with times of flight τ of the order of 1 ns and a Rabi frequency Ω_0 and excitation rate γ_0 which correspond to typical laser intensities of the order of $10^7 - 10^8$ W cm^{-2} in the case of sodium atoms, for example. As may be seen from Fig. 2(a) these parameters imply an efficiency of the beam splitter of the order of 30%. As in the case of other atomic beam splitters [4] the Raman-Nath condition $kLP_x/P_{in} \ll 2\pi$ places an upper limit on the maximum momentum splitting, which can be predicted reliably within our model (for sodium atoms, for example, with $v_{in} = 1000$ ms^{-1}, $L = 5$ μm, and $\lambda = 2\pi/k = 600$ nm, $kLP_x/P_{in} \approx (P_x/\hbar k)2.5 \times 10^{-3}$ is found). In order to achieve a large momentum transfer within the validity of the Raman-Nath approximation, a large spatial period of the standing-wave laser field is desirable. Such large periods, which are significantly larger than the wavelength of the laser field $\lambda = 2\pi c/\omega$ (c is the speed of light), can be produced, for example, by crossing two laser beams at a small angle [2,15,16]. Furthermore, it should be taken into account that experimental imperfections such as an initial velocity spread of the atomic beam or effects of a more realistic (nonrectangular) envelope of the laser field will tend to broaden the momentum distributions shown in Figs. 2(b–d) slightly.

[1] P. J. Martin, B. G. Oldaker, A. H. Miklich, and D. E. Pritchard, Phys. Rev. Lett. **60**, 515 (1988).

[2] T. Sleator, T. Pfau, V. Balykin, O. Carnal, and J. Mlynek, Phys. Rev. Lett. **68**, 1996 (1992).

[3] G. Timp, R. E. Behringer, D. M. Tennant, J. E. Cunningham, M. Prentiss, and K. K. Berggren, Phys. Rev. Lett. **69**, 1636 (1992).

[4] T. Pfau, C. S. Adams, and J. Mlynek, Europhys. Lett. **21**, 439 (1993); C. S. Adams, T. Pfau, Ch. Kurtsiefer, and J. Mlynek, Phys. Rev. A **48**, 2108 (1993).

[5] S. Nic Chormaic, V. Wiedemann, Ch. Miniatura, J. Robert, S. Le Boitex, V. Lorent, O. Goceix, S. Fernon, J. Reinhardt, and J. Baudon, J. Phys. B **26**, 1271 (1993).

[6] P. Marte, P. Zoller, and J. L. Hall, Phys. Rev. A **44**, R4118 (1991).

[7] M. A. M. Marte, J. I. Cirac, and P. Zoller, J. Mod. Opt. **38**, 2265 (1991).

[8] S. Dyrting and G. J. Milburn, Phys. Rev. A **47**, R2484 (1993).

[9] A survey of recent work is given in Appl. Phys. B **54**, 321 (1992).

[10] A. P. Kazantsev, G. A. Ryabenko, and G. I. Surdutovich, Phys. Rep. **129**, 75 (1985).

[11] G. Alber, Phys. Rev. Lett. **69**, 3045 (1992); **70**, 2200 (1993).

[12] G. Alber and P. Zoller, Phys. Rep. **199**, 231 (1991).

[13] Without effects of atomic motion a similar model has been discussed previously by G. Alber, Th. Haslwanter, and P. Zoller, J. Opt. Soc. Am. B **5**, 2439 (1988).

[14] M. J. Seaton, Rep. Prog. Phys. **46**, 167 (1983).

[15] R. G. De Voe, Opt. Lett. **16**, 1605 (1991).

[16] D. M. Giltner, R. W. Mc Gowan, N. Melander, and S. A. Lee, Opt. Commun. **107**, 227 (1994).